جامعة الملك عبدالله
للعلوم والتقنية
King Abdullah University of
Science and Technology

Accelerating vapor condensation with daytime radiative cooling

Item Type	Conference Paper
Authors	Zhou, Ming;Song, Haomin;Xu, Xingyu;Shahsafi, Alireza;Xia, Zhenyang;Ma, Zhenqiang;Kats, Mikhail A.;Zhu, Jia;Ooi, Boon S.;Gan, Qiaoqiang;Yu, Zongfu
Citation	Zhou, M., Song, H., Xu, X., Shahsafi, A., Xia, Z., Ma, Z., ... Yu, Z. (2019). Accelerating vapor condensation with daytime radiative cooling. New Concepts in Solar and Thermal Radiation Conversion II. doi:10.1117/12.2525125
Eprint version	Post-print
DOI	10.1117/12.2525125
Publisher	SPIE-Intl Soc Optical Eng
Rights	Archived with thanks to SPIE
Download date	2024-04-20 10:47:21
Link to Item	http://hdl.handle.net/10754/632521

Accelerating vapor condensation with daytime radiative cooling

Ming Zhou[1], Haomin Song[2], Xingyu Xu[3], Alireza Shahsafi[1], Zhenyang Xia[1], Zhenqiang Ma[1], Mikhail Kats[1], Jia Zhu[4], Boon S. Ooi[5], Qiaoqiang Gan[2, †], Zongfu Yu[1, *]

1. Department of Electrical and Computer Engineering, University of Wisconsin – Madison, Madison, WI 53705, USA
2. Department of Electrical Engineering, The State University of New York at Buffalo, Buffalo, NY 14260, USA
3. School of Materials Science and Engineering, Tsinghua University, Beijing 100084, China
4. College of Engineering and Applied Sciences, Nanjing University, Nanjing 210093, China
5. Photonics Laboratory, King Abdullah University of Science and Technology (KAUST), Thuwal, 23955-6900, Saudi Arabia

† Correspondence to: Qiaoqiang Gan (qqgan@buffalo.edu)

* Correspondence to: Zongfu Yu (zyu54@wisc.edu)

Evolution has produced many ingenious surviving techniques for animals living in extreme arid environment. One of them is to produce water from thin air. Darkling beetles in the Namib desert collect water droplets and generate dew from the moisture-rich breeze blown in from the Atlantic. The key to dew generation is the color of beetle body, which sheds thermal energy efficiently and functions as a cooling source for water condensation. However, this fascinating water-generation technique only works around dawn before the sun gets its full strength, after which the black surface quickly heats up by sunlight absorption and becomes an evaporator instead of a condenser. Inspired by Namib beetles, we develop passive radiative condensers that take zero energy input and create dew water at the room temperature. To overcome the challenge faced by beetles, we designed the thermal radiators to reflect solar radiation while efficiently dissipating heat through radiation so that water can be efficiently condensed under sunlight.

Introduction

Energy and clean water are global challenges that are intertwined in a rather unfavorable way: even in areas where water is available, energy may not be available to clean water for human use(*1*, *2*). Decoupling the energy and water can bring substantial benefits to billions of people living in areas where the lack of energy limits the access to clean water(*3*). In this context, there has been strong interest in developing passive clean water technology that does not actively consume energy. Solar clean water technology is particularly promising because solar energy is abundant and widely accessible. The solar still, which uses sunlight to evaporate and purify water, has a long history(*4–6*). Recently, advances in nanoscale engineering has substantially improved its effectiveness (*7*). Much progress has been made to reduce the cost of solar absorber(*8*) and to improve the evaporation efficiency (*9*, *10*). Related to solar still, sunlight has been used to harvest atmospheric vapor by evaporating vapor collected in a porous metal-organic framework(*11*).

These solar water purification technologies involve two energy sources: a heating source for evaporation and a cooling source for condensation. Most recent works have focused on using sunlight as efficient heating sources(*7–10*), where the one-sun evaporation efficiency is already approaching the theoretical limit of ~ 1.6 $L\ m^{-2}\ hour^{-1}$(*12*). On the other hand, the equally important condensation efficiency has been mostly neglected. Most previous research in condensation has focused on surface hydrophilicity(*13*), which does not address the fundamental issue of cooling. As we will show, passive cooling sources including convection and conduction could not prove sufficient cooling power. Its power is lower than the heating power of sunlight. The difference results in mismatched evaporation and condensation rates, which consequently pins the water production rate to a rate much less than the theoretical limit(*6*).

Here we exploit the universe as the free coldness reservoir for water condensation. We access the coldness of the universe via radiative energy exchange(*14*) made possible by the atmospheric-transparency window in mid-infrared spectral range from 8 to13 μm. This cooling source is used by beetles to condense water from air at nighttime(*15*). Recently, Fan et. al showed that sub-ambient cooling can be realized even during the daytime(*16*). Building upon these work, we show a daytime radiative condenser. Compared to traditional passive condensers, it offers the following key advantages: first, the daytime radiative condenser provides effective condensation for vapor at ambient temperature when conduction and convection fail to condense water. Secondly, compared to traditional radiative condensers(*13*, *17*, *18*) our condenser can function even in the presence of sunlight, which is essential to be used in solar still systems that mainly operate during daytime. Lastly, when used for solar still, it provides substantial cooling power that can more than double the condensation rate. The resulting condensation rate can match the evaporation rate to realize efficient phase-change water cleaning/production systems.

Results

Water vapor condenses when its temperature drops below the dew point. For the case of Namib beetles(*15*), the vapor in air is at ambient temperature, and the dew point is slightly lower than the ambient temperature. The cooling can only be provided by thermal radiation because the conduction and convection would work against cooling below ambient temperature. The black

body of the beetles emits infrared radiation strongly around the atmospheric-transparency window (8-13 μm). In this spectral region, the atmosphere is transparent and does not emit back to the beetle. Only radiation from the universe emits back to the beetle, but it carries very little thermal energy because of its low temperature of 3 K. Consequently, the Namib beetle can passively dissipate heat through the atmospheric-transparency window to the universe, cooling down itself below the dew point. This cooling mechanism has been commercialized to build radiative dew water condensers, which can produce water at rates(*17*, *18*) of 0.03~0.06 $L\ m^{-2}\ hour^{-1}$ when assuming 10 hours of working time at night.

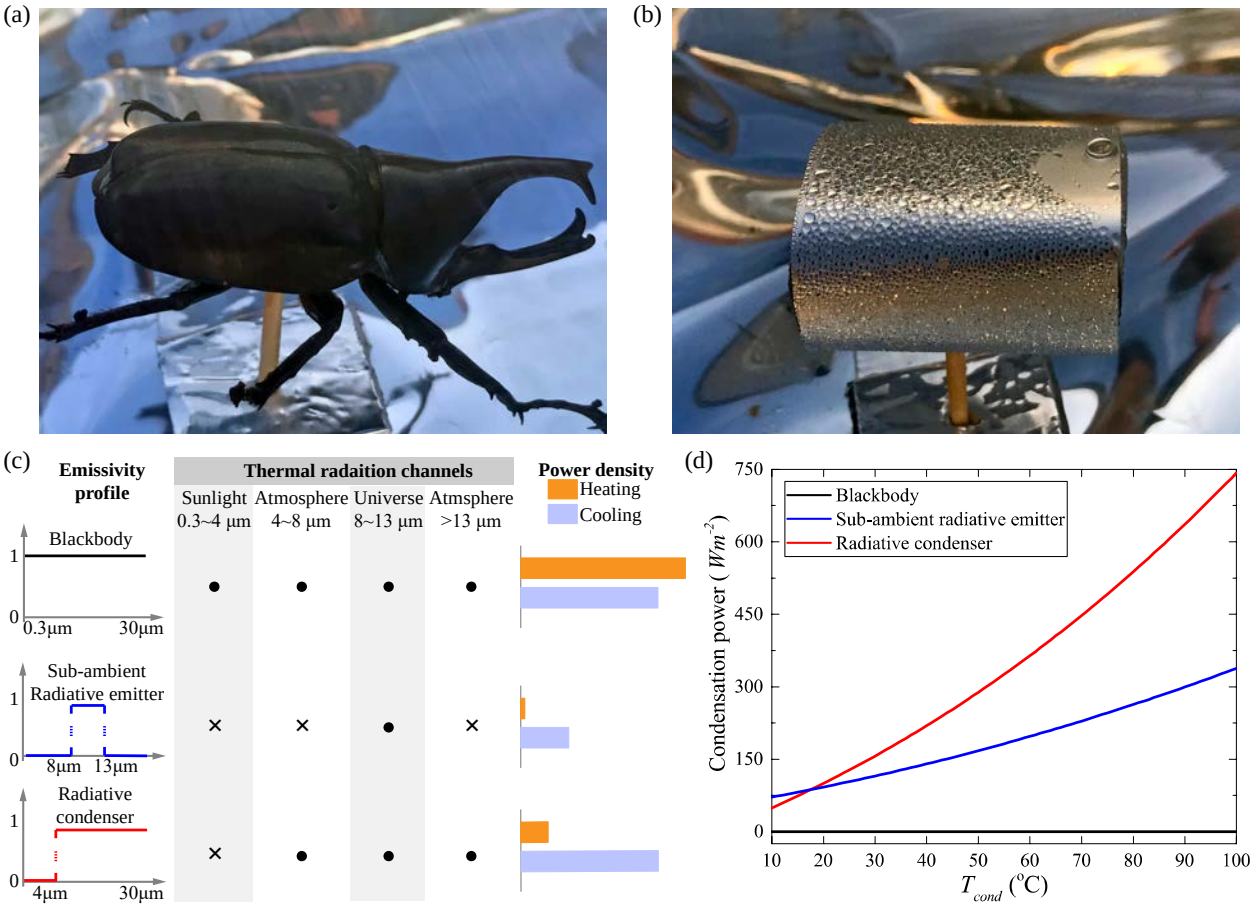

Figure 1. Pictures of (a) darkling beetle and (b) our artificial beetle. Both were placed under direct sunlight, with 90% ~95% humidity air blowing towards them at the same speed. The darkling beetle does not condense vapor due to its absorption of sunlight. In contrast, our artificial beetle reflects most of the sunlight as indicated by its shining surface. It condenses water vapor during daytime and generates dew water. (c) Thermal radiation channels and emissivity spectra of blackbody (black), sub-ambient radiative emitter (blue) considered in Ref [14] and radiative condenser (red). The spectrum of environment radiation is divided into four channels - the solar channel (0.3~4 μm), the universe channel (8~13 μm) and the atmospheric channels (4~8 μm and >13 μm). The dot (cross) indicates that the emitter has the corresponding channel open (close) for heat exchange. The heating and cooling power density of the emitters are plotted as orange and blue bars, respectively. The blackbody has all channels open and receives more heat than it can radiate under sunlight. The sub-ambient radiative emitter has only the universe channel open. It receives lowest heat but also radiates much least amount of heat. The radiative condenser only closes the solar channel and radiates much more heat than it receives. (d) Condensation power of the emitters operating at different temperatures. The ambient

temperature is fixed at 20 ºC. The blackbody (black) has zero condensation power. The radiative condenser (red) has much more condensation power than the sub-ambient radiative emitter (blue).

Both the Namib beetle and commercial dew condensers only work before sun is at full strength. As the sun rises, the heat absorbed due to sunlight radiation(*12*) reaches 1000 $W\,m^{-2}$, much stronger than the radiative cooling power. As a result, no cooling can be achieved at daytime. By spectrally engineering the absorptivity, one can block the absorption of sunlight in the visible and near-IR regions while maintaining excellent thermal radiation in the mid-IR regions(*16*, *19*). By preventing solar absorption, such a condenser can be made to work during both the day and night. Figure 1 shows two artificial beetles under direct sunlight. The black one mimics the natural black beetle than condenses vapor around dawn. The other one (Fig. 1b) reflects most of the sunlight but emits efficiently outside the solar spectrum. When vapor at ambient temperature flows through both "beetles" during daytime, the black beetle does not condense water vapor due to its absorption of sunlight. In contrast, visible water droplets can be seen on our daytime condensing beetle.

Now we explain the design principle of the radiative condenser. The key is to spectrally engineer radiative surface to enable or disable specific heat exchange channels with the environment. The spectrum of the environment radiation can be divided into four segments as shown in Fig. 1c. In the wavelength range 0.3 to 4 μm, the incoming radiation is dominated by the solar radiation. The incoming heat power flux in this channel is around 1000 Wm^{-2}. From 4 to 8 μm, it is dominated by atmospheric radiation. For an ambient temperature of 20 ºC, its power is 50 Wm^{-2}. From 8~13 μm, the only incoming radiation is from the universe under clear sky, which is about 40 W m^{-2}. Beyond 13 μm, incoming radiation is again dominated by atmospheric radiation, carrying a power of 130 W m^{-2}. The radiation power flux in these channels are calculated as $q = \int d\Omega\, cos\theta \int_{\lambda_1}^{\lambda_2} d\lambda\, I_{BB}(T_{amb}, \lambda)\epsilon_{atm}(\lambda, \theta)$, where $I_{BB}(T_{amb}, \lambda)$ is the spectral irradiance of a blackbody at ambient temperature T_{amb}. The angle dependent emissivity of atmosphere is given by(*20*) $\epsilon_{atm}(\lambda, \theta) = 1 - t(\lambda)^{1/\cos\theta}$, where $t(\lambda)$ is the atmospheric transmittance in the zenith direction(*21*).

A blackbody has all four channels open for heat exchange as shown in Fig. 1c. Because of the strong solar radiation, it receives more radiative heat than it can radiate. A blackbody has no cooling power, even for vapor at 100 ºC (Fig. 1d). Daytime sub-ambient radiative emitter as considered in (*16*, *19*) is realized by closing all channels except for the universe. The radiation heat received is substantially reduced, to as low as 40 $W\,m^{-2}$, allowing cooling well below ambient temperature(*22*). However, as it closes most of the radiative channels, the amount of the heat it can radiate is also reduced. This design is sub-optimal for a radiative condenser. Our radiative condensers only close the solar channel and leave the atmospheric channels completely open as shown in Fig. 1c. This design is undesirable for sub-ambient cooling(*23*). However, the vapor created by in most water application is at or above the ambient when an open atmospheric channel can substantially contribute to cooling. As shown in Fig. 1d, radiative condensers (red line) more than double the cooling power when compared to sub-ambient radiative emitters (red line) at most vapor temperatures of practical relevance.

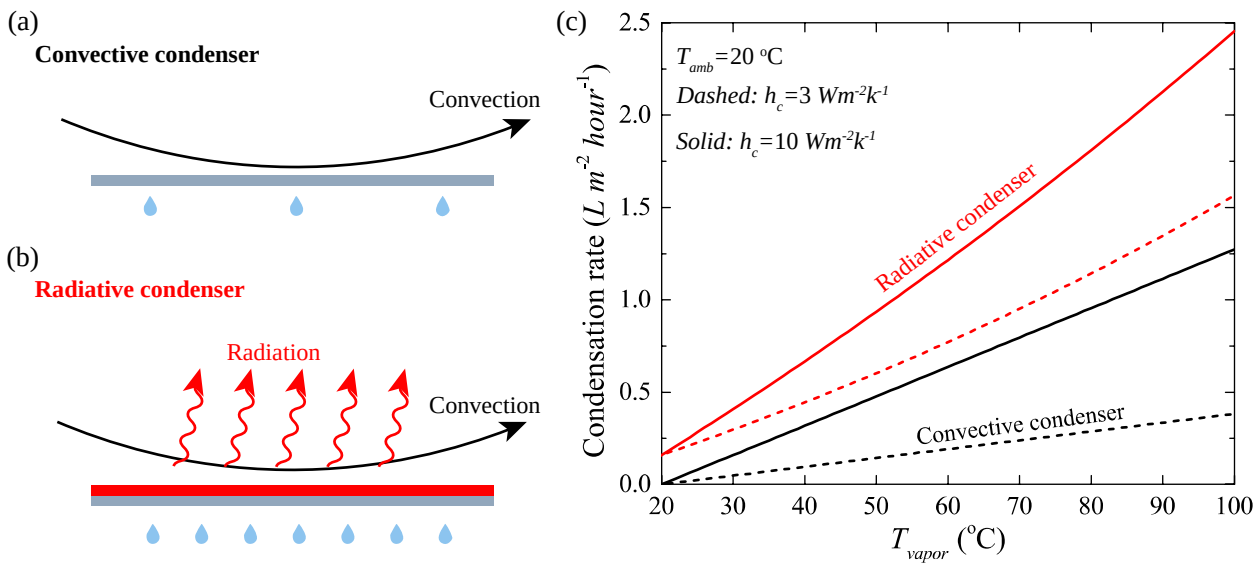

Figure 2. (a) and (b) Schematic of convective passive condenser (a) and radiative passive condenser (b). The convective condenser dissipates heat through only convection, and the radiative condenser dissipates heat through both convection and radiation. (c) Theoretically calculated condensation rates of connective (black) and radiative condenser (red). The ambient temperature is fixed at 20 °C and the relative humidity of input air flow is fixed at 100%.

Next, we discuss the application of daytime radiative condenser in solar still systems. We developed a theoretical model to calculate the steady-state condensation rates. The details of the theoretical model are available in Section 1 of Supplementary Materials.

Water vapor created by sunlight absorption can condense through natural convection (Fig. 2a) because the vapor temperature T_{vapor} is often above the ambient temperature T_{amb}. The cooling power can be calculated as $P_{conv} \cong h_c(T_{vapor} - T_{amb})$, where h_c is the convective heat transfer coefficient. h_c depends on the wind speed at the surface of the condenser, which usually ranges from 3 to 10 $\mathrm{Wm^{-2}K^{-1}}$ for wind speed from 0 to 10 mph without considering surface friction(*24*). The condensation rate can be calculated from the cooling power as $W_{water} = P_{conv}/\Delta_{vapor}$, where $\Delta_{vapor} = 2.26 \times 10^6\ J\ kg^{-1}$ is the latent heat from vapor to liquid. Even in the situation most favorable for convection cooling, e.g. vapor at 100 °C temperature and with a wind speed of 10 mph (black solid curve in Fig. 2b), the condensation rate is only 1.3 $L\ m^{-2}\ hour^{-1}$. This rate is below the limit of one-sun vapor generation rate(*12*) of 1.6 $L\ m^{-2}\ hour^{-1}$. The situation became much worse when there is no wind (black dashed curve in Fig. 2b). In most practical situation, the vapor temperature is well below 100 °C. For instance, the temperature of water vapor in the solar still in Ref. [8]., which was demonstrated to have the highest solar-to-thermal efficiency, is only 40 °C. At such low temperature, the theoretical upper bounds of the condensation rates of convective condenser are less than 0.1 $L\ m^{-2} hour^{-1}$. Such low condensation rate becomes the bottleneck of water production in solar-based water technologies. Daytime radiative condenser can effectively improve the condensation rate across all temperature range. Even at low temperature, e.g. 40 °C., the condensation rates without wind are enhanced by more than 4 times, to 0.44 $L\ m^{-2} hour^{-1}$. At high temperatures, e.g. 100 °C, the condensation rate almost doubles, reaching 2.5 $L\ m^{-2}\ hour^{-1}$, well above the limit of solar evaporation rate. Such high condensation rate will help to increase vapor-pressure gradient inside a solar still, facilitating the evaporation process.

We now describe the experimental realization of radiative condensers. Figure 3a shows the schematic of the radiator designed to approach the near-ideal condenser spectrum (black dashed line). It consists of layers of polydimethylsiloxane (PDMS) and silver (Ag) and an aluminum (Al) substrate, with thickness of 100 μm, 150 nm and 1 mm, respectively. The radiation mainly arises from the PDMS layer, which has a near-unity emissivity for wavelengths longer than 4.5 μm due to Si–O and Si–C bond vibrations(*25*). PDMS is transparent to sunlight, which can be reflected by the underneath Ag layer. The Al substrate is chosen because of its high thermal conductivity. The width and length of the condensation region are 25 cm and 20 cm, respectively. The emissivity of the structure is characterized using Fourier transform infrared spectroscopy and the measured emissivity spectrum is shown in Fig. 3a. Our daytime radiative condenser reflects almost 96% of the solar radiation (0.3~4 μm) and emits efficiently in mid-IR region (>4 μm). We then place the radiator inside an insulating box made from polystyrene as shown in Fig. 3b. The external surface of the insulating box is covered with aluminized foil tape to prevent solar heating. A low-density polystyrene film covers the opening of the insulating box to reduce convective heat losses.

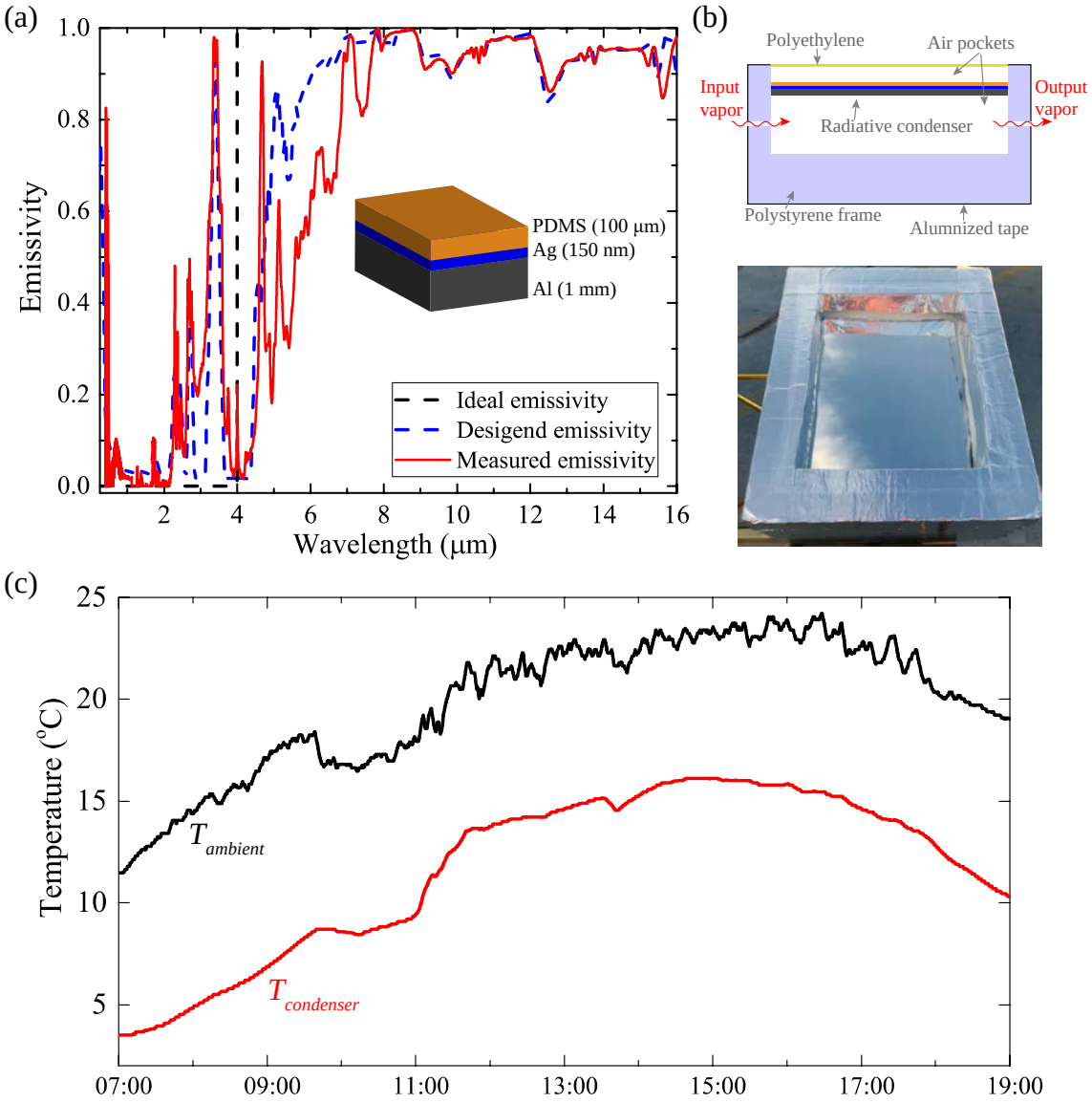

Figure 3. Experimental design of daytime radiative condenser. (a) Schematic of the daytime radiative emitter and measured emissivity spectrum. The emitter consists of a 100 μm thick layer of PDMS, a 150 nm thick layer of silver and a 1 mm thick aluminum plate. (b) Experimental setup of the daytime radiative condenser. The emitter is placed inside an insulating polystyrene box. The opening of the insulating box is covered by a thin polyethylene film and the external surface of the box is covered by aluminized foil tape. (c) Daytime cooling power under direct sunlight. The temperature of the condenser is about 8 ºC lower than the ambient temperature throughout the day.

To characterize the cooling power of our radiative condenser under direct sunlight, we placed it on a roof facing the sky. The temperature of the condenser is measured by attaching a thermocouple at center of the backside of the condenser with conductive tape. The temperature of the ambient air is measured by placing a thermocouple inside a weather shield to avoid sunlight and wind. The measurement was performed on a sunny day with clear sky from 07:00 to 19:00. Figure 3c shows the temperature of the condenser (red curve) and the ambient air (black curve), as well as the calculated cooling power (blue curve). The temperature of the condenser is about 8 ºC lower than the ambient temperature throughout the day, which is similar to that of existing sub-ambient radiative emitters(*16*, *19*).

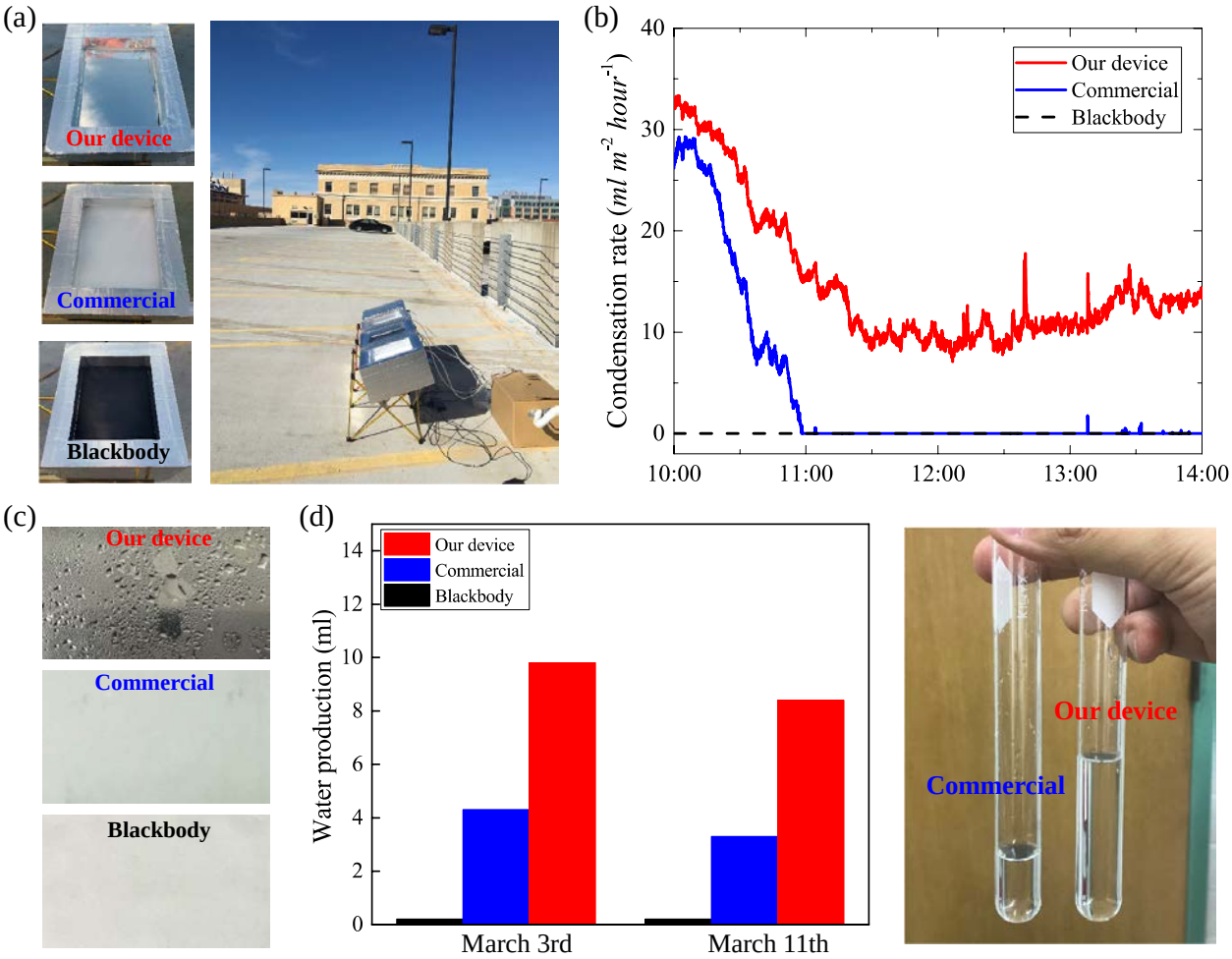

Figure 4. (a) Left: front-side pictures of condensers used for measurement. A blackbody and commercial condenser are used for comparison. Right: Outdoor experimental setup. The condensers are placed on top floor of a parking ramp under direct sunlight. (b) Real-time condensation rates of our daytime radiative condenser (red line), commercial

radiative condenser (blue line) and blackbody radiative condenser (black line). The measurement was performed from March 10th to 11th. Here for simplicity, we only plot data recorded during daytime on March 10th. The blackbody had zero condensation rate due to absorption of sunlight. The commercial condenser initially had non-zero condensation rate in the morning as absorbs less sunlight, but eventually stropped to work around noon, i.e. condensation rate dropped to zero. Our daytime condenser always had non-zero condensation rate during the daytime. (c) Pictures of the condensing surface for each condenser at noon, March 11th. Visible water droplets can only be seen on our daytime radiative condenser. (d) Daily water productions measured at two different days. The picture on the right shows a visual comparison between the amount of water produced by our device and the commercial nighttime condenser.

Next, we show day-time condensation for vapor at ambient temperature. At this temperature, traditional passive cooling mechanisms such as conduction and convection are completely ineffective.

Two additional condensers were used for comparison: one blackbody emitter and one commercial nighttime radiative condenser(*26*) as shown in Fig. 4a. The blackbody emitter made of graphite is coated an Al plate with the same dimensions with our radiative condenser. The commercial condenser consists a white low-density polyethylene foil, with 5% volume of TiO_2 nanoparticles (diameter 0.19 μm) and 5% volume of $BaSO_4$ nanoparticles (diameter 0.8 μm). This material is a standard material for nighttime radiative condensation recommended by the International Organization for Dew Utilization(*13*, *27*). As we will show below, it does not condense room-temperature vapor under sunlight. We also attached the commercial condenser to an Al plate with the same dimensions with our radiative condenser. In addition to those condensers, a reference device consists of a plain Al plate was used to measure the ambient temperature and humidity of the input air flow.

All condensers were then placed on a roof facing the sky. Humified air with a relative humidity of 90%~95% was pumped into all condensers at a constant rate of $V_{in} = 0.9\ m^3\ hour^{-1}$. The vapor is filtered through water trap to ensure no water droplet is contained in the vapor entering the cooling chamber. We then performed day-to-night measurements in March of 2018. The temperature T_{out} and relative humidity H_{out} of the output air flow were measured by directly attaching a temperature and relative humidity probe at the output outlet. The amount of water contained in the output air flow then was directly obtained as $m_{out} = H_{out}P(T_{out})V_{in}M_{water}/R$, where $P(T)$ is the vapor pressure at temperature T, R is the ideal gas constant and M_{water} is the molar mass of water. The vapor pressure $P(T)$ was calculated using Buck equation(*28*). The condensation rate then was obtained as $W_{cond} = (m_{in} - m_{out})/\mathrm{A_{cond}}$, where m_{input} is the amount of water contained in the input air flow and A_{cond} is the area of the condensers. The overall water production of the condensers was further obtained by measuring the weight change of the condensers.

Figure 4b shows a typical measurement during daytime. The blackbody absorbs almost all the sunlight and does not condense vapor as indicated by its zero-condensation rate (black curve). The commercial condenser absorbs less sunlight. It condensed vapor in the morning when sunlight was weak. As sunlight got its full strength around noon, the condensation rate of the commercial condenser (blue curve) also dropped to zero. In contrast, our daytime condenser continued to condense water vapor even at noon. Figure 4c shows pictures of the back surface of the condensers before sunset. The vapor flows below the condensing surface. Water droplets can be seen on the

back surface of our daytime radiative condenser. The water production over day-to-night periods further confirms the daytime condensation of our daytime condenser. As shown in Fig. 4d, the water production of our daytime radiative condenser is almost twice that of the commercial condenser. On the other hand, the water production of the blackbody condenser was almost zero because the water condenses at night is evaporated during daytime.

A radiative condenser can also be designed to be transparent to solar radiation. Such a radiative condenser provides similar condensation performance and can be directly integrated with existing solar stills. An example of transparent radiative condenser is given in Section 2 of Supplementary Materials.

In conclusion, we show that daytime radiative condenser can significantly accelerate the condensation of vapor. We experimentally demonstrated water condensation of ambient-temperature vapor under sunlight. Such effective water condensation cannot be realized by either conventional radiative condensers, or natural convention condensers. By extending the operation to daytime, the radiative condenser could be very useful for solar-based clean-water technologies. In these passive system, the cooling power is generally lower than the solar heating power, creating the imbalance of evaporation and condensation rates. The imbalance consequently decreases the overall water production rate. Daytime radiative condensers provide much-needed passive cooling source to effective remove the imbalance, paving the way to highly efficient solar still systems.

References

1. M. A. Shannon *et al.*, Science and technology for water purification in the coming decades. *Nature*. **452**, 301–310 (2008).

2. M. Elimelech, W. A. Phillip, The Future of Seawater Desalination: Energy, Technology, and the Environment. *Science*. **333**, 712–717 (2011).

3. D. Molden, Ed., *Water for Food Water for Life: A Comprehensive Assessment of Water Management in Agriculture* (Routledge, London ; Sterling, VA, 2007).

4. H. E. S. Fath, Solar distillation: a promising alternative for water provision with free energy, simple technology and a clean environment. *Desalination*. **116**, 45–56 (1998).

5. S. A. Kalogirou, Seawater desalination using renewable energy sources. *Progress in Energy and Combustion Science*. **31**, 242–281 (2005).

6. M. Ali Samee, U. K. Mirza, T. Majeed, N. Ahmad, Design and performance of a simple single basin solar still. *Renewable and Sustainable Energy Reviews*. **11**, 543–549 (2007).

7. H. Ghasemi *et al.*, Solar steam generation by heat localization. *Nature Communications*. **5**, 4449 (2014).

8. Z. Liu *et al.*, Extremely Cost-Effective and Efficient Solar Vapor Generation under Nonconcentrated Illumination Using Thermally Isolated Black Paper. *Global Challenges*. **1**, 1600003 (2017).

9. L. Zhou *et al.*, 3D self-assembly of aluminium nanoparticles for plasmon-enhanced solar desalination. *Nature Photonics*. **10**, 393–398 (2016).

10. F. Zhao *et al.*, Highly efficient solar vapour generation via hierarchically nanostructured gels. *Nature Nanotechnology*, 1 (2018).

11. H. Kim *et al.*, Water harvesting from air with metal-organic frameworks powered by natural sunlight. *Science*, eaam8743 (2017).

12. G. Ni *et al.*, Steam generation under one sun enabled by a floating structure with thermal concentration. *Nature Energy*. **1**, 16126 (2016).

13. B. Khalil *et al.*, A review: dew water collection from radiative passive collectors to recent developments of active collectors. *Sustain. Water Resour. Manag.* **2**, 71–86 (2016).

14. E. Rephaeli, A. Raman, S. Fan, Ultrabroadband Photonic Structures To Achieve High-Performance Daytime Radiative Cooling. *Nano Lett.* **13**, 1457–1461 (2013).

15. J. Guadarrama-Cetina *et al.*, Dew condensation on desert beetle skin. *Eur. Phys. J. E*. **37**, 109 (2014).

16. A. P. Raman, M. A. Anoma, L. Zhu, E. Rephaeli, S. Fan, Passive radiative cooling below ambient air temperature under direct sunlight. *Nature*. **515**, 540–544 (2014).

17. M. Muselli *et al.*, Dew water collector for potable water in Ajaccio (Corsica Island, France). *Atmospheric Research*. **64**, 297–312 (2002).

18. J. F. Maestre-Valero, V. Martínez-Alvarez, A. Baille, B. Martín-Górriz, B. Gallego-Elvira, Comparative analysis of two polyethylene foil materials for dew harvesting in a semi-arid climate. *Journal of Hydrology*. **410**, 84–91 (2011).

19. Y. Zhai *et al.*, Scalable-manufactured randomized glass-polymer hybrid metamaterial for daytime radiative cooling. *Science*, eaai7899 (2017).

20. C. G. Granqvist, A. Hjortsberg, Radiative cooling to low temperatures: General considerations and application to selectively emitting SiO films. *Journal of Applied Physics*. **52**, 4205–4220 (1981).

21. S. D. Lord, "A new software tool for computing Earth's atmospheric transmission of near- and far-infrared radiation" (1992), (available at https://ntrs.nasa.gov/search.jsp?R=19930010877).

22. Z. Chen, L. Zhu, A. Raman, S. Fan, Radiative cooling to deep sub-freezing temperatures through a 24-h day–night cycle. *Nature Communications*. **7**, 13729 (2016).

23. J. Kou, Z. Jurado, Z. Chen, S. Fan, A. J. Minnich, Daytime Radiative Cooling Using Near-Black Infrared Emitters. *ACS Photonics*. **4**, 626–630 (2017).

24. J. H. Watmuff, W. W. S. Charters, D. Proctor, "Solar and wind induced external coefficients - Solar collectors" (1977), p. 56.

25. D. K. Cai, A. Neyer, R. Kuckuk, H. M. Heise, Optical absorption in transparent PDMS materials applied for multimode waveguides fabrication. *Optical Materials*. **30**, 1157–1161 (2008).

26. T. M. J. Nilsson, G. A. Niklasson, Radiative cooling during the day: simulations and experiments on pigmented polyethylene cover foils. *Solar Energy Materials and Solar Cells*. **37**, 93–118 (1995).

27. International Organization For Dew Utilization, (available at http://www.opur.fr/).

28. A. L. Buck, New Equations for Computing Vapor Pressure and Enhancement Factor. *J. Appl. Meteor.* **20**, 1527–1532 (1981).

Supplementary Materials

Section 1. Steady-state model of passive condensation systems

We developed a steady-state model to calculate the condensation rate of passive condensation systems. Below we will describe it in detail.

As we discussed in the manuscript, the major cooling sources in passive condensers that operate without additional energy input are convection and radiation. The convective cooling flux q_{conv} and radiative cooling flux q_{rad} are given by

$$q_{conv}(T_{cond}) = h_c(T_{cond} - T_{amb}) \tag{1}$$

$$q_{rad}(T_{cond}) = \int d\Omega \, cos\theta \int_0^{+\infty} d\lambda \, I_{BB}(T_{cond}, \lambda)\epsilon_{cond}(\lambda, \theta) \tag{2}$$

Here h_c is the convective heat transfer coefficient, T_{cond} and T_{amb} are the temperature of the condenser and the surrounding environment, respectively. $I_{BB}(T, \lambda)$ is the spectral intensity of a blackbody at temperature T. $\epsilon_{cond}(\lambda, \theta)$ is the spectral emissivity of the condenser.

The major heating sources are the solar radiation and atmospheric radiation, whose heating flux are given by

$$q_{solar} = \int d\Omega \, cos\theta \int_0^{+\infty} d\lambda \, I_{AM1.5}(\lambda)\epsilon_{cond}(\lambda, \theta) \tag{3}$$

$$q_{atm} = \int d\Omega \, cos\theta \int_0^{+\infty} d\lambda \, I_{BB}(T_{amb}, \lambda)\epsilon_{cond}(\lambda, \theta)\epsilon_{atm}(\lambda, \theta) \tag{4}$$

Here $I_{AM1.5}(\lambda)$ are the AM1.5 solar spectral irradiance. We assume the atmosphere is at ambient temperature throughout our calculation. The angle dependent emissivity of atmosphere is given by(*1*) $\epsilon_{atm}(\lambda, \theta) = 1 - t(\lambda)^{1/\cos\theta}$, where $t(\lambda)$ is the atmospheric transmittance in the zenith direction(*2*).

As humidified air with a temperature of T_{input} and a humidity of $H_{relative}$ flows through the condenser, it's cooled down and the vapor pressure drops. Condensation occurs when the vapor pressure reaches the saturation vapor pressure. We approximated the saturation vapor pressure $P(T)$ at temperature T using the Buck equation(*3*)

$$P(T) = 611.21 \exp\left(\left(18.678 - \frac{T - 273.15}{234.5}\right)\left(\frac{T - 273.15}{T - 16.01}\right)\right) \tag{5}$$

The amount of heat flux required for condensation of vapor and cooling down the input air flow are the given by

$$q_{vapor}(T_{cond}) = u\Delta_{vap}\left(\frac{H_{relative}P(T_{in})}{RT_{input}} - \frac{P(T_{cond})}{RT_{cond}}\right) \tag{6}$$

$$q_{air}(T_{cond}) = C_{V,air}u(T_{cond} - T_{in}) \tag{7}$$

where u is the speed of the input air flow at the air-condenser interface and R is the ideal gas constant. The latent heat from vapor to liquid water is given by Δ_{vap}= 40.63 kJ/mol and $C_{V,air}$ is the specific heat capacity of air at constant volume.

At steady state, the whole system reaches thermal equilibrium, which satisfies

$$q_{conv}(T_{cond}) + q_{rad}(T_{cond}) - q_{solar} - q_{atm} = q_{vapor}(T_{cond}) + q_{air}(T_{cond}) \tag{8}$$

By solving Eq. 8, we obtain the working temperature of the condenser T_{cond}, which depends on the input humidity $H_{relative}$ and air flow rate u. The condensation rate of the condenser then can be calculated as

$$W_{water} = \frac{q_{vapor}}{\Delta_{vap}} M_{water} \tag{9}$$

where M_{water} is the molar mass of water.

To validate our theoretical model, we predict the condensation rate of our condenser based on measured T_{in}, T_{amb} and H_{in}, and compare it to the measurement. The measurement was performed from March 10th to 11th. The input air flow rate $u = 0.025\ m/s$. The convective heat transfer coefficient h_{conv} is taken to be 6 $Wm^{-2}K^{-1}$. The results are plotted in Fig. S1. The predicted condensates (red curve) fits the measurement (black curve) very well. Here for simplicity, we consider nighttime condensation where the solar radiation is completely suppressed, i.e. $q_{solar} = 0$.

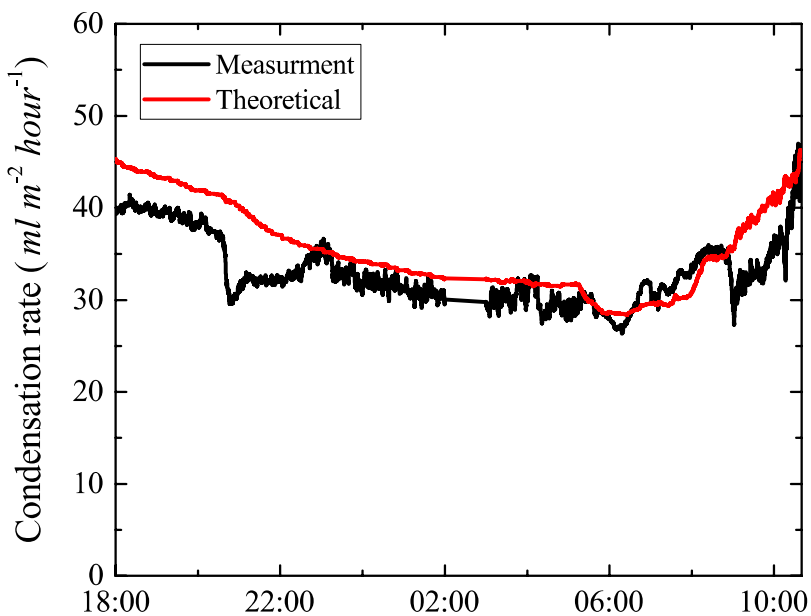

Figure S1. The theoretically predicated condensation rates (red) fits the experimental measurements (black) very well.

Section 2. Transparent daytime radiative condenser

Here we propose a simple design of transparent daytime radiative condenser that can be readily implemented in existing solar stills. As shown in Fig. S2a, the transparent radiative condenser consists of a thin layer of PDMS on top of glass, with a thickness of 100 μm. Figure S2b shows the transmission (red curve) and emissivity (black curve) spectra of the PDMS-glass condenser. It barely affects the solar evaporation rates as more than 93% of solar radiation can pass through it. More importantly, it still emits efficiently with a near-unity emissivity in the mid-IR region. As a result, it has similar radiative condensing performance as the daytime radiative condenser described in Fig. 4 in the manuscript.

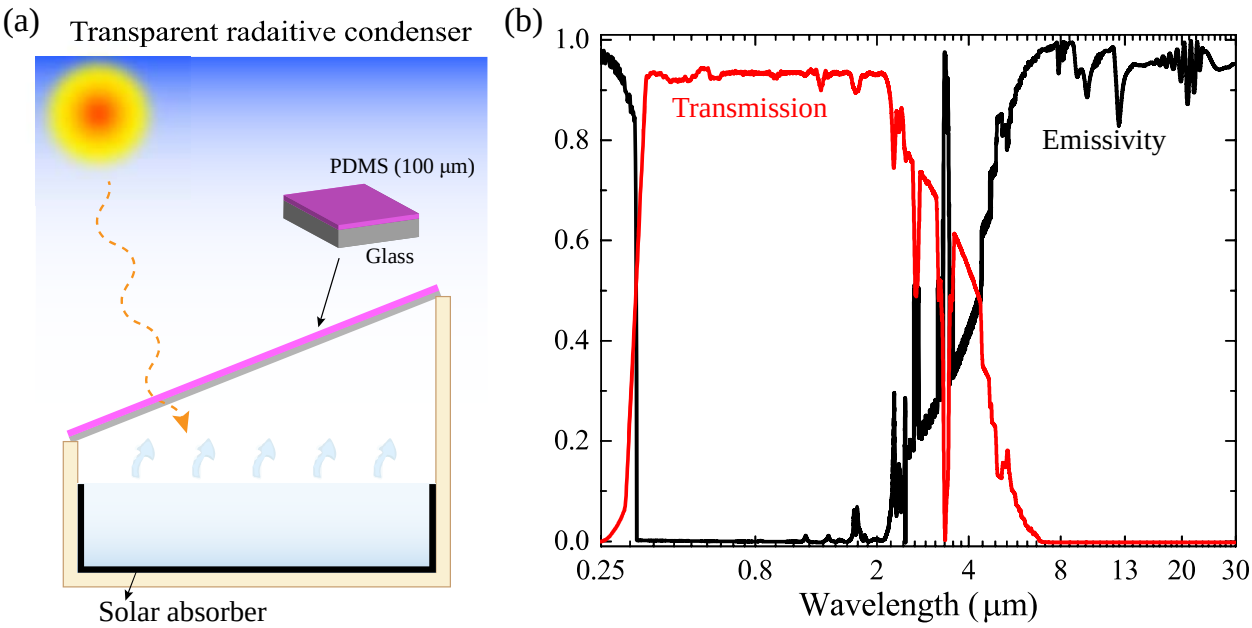

Figure S2. Transparent radiative condenser. (a) The transparent condenser can be readily implemented in existing solar stills. It consists of a layer of PDMS with a thickness of 100 μm, on top of a glass substrate. (b) Transmission (red) and emissivity (black) spectra.

References

1. C. G. Granqvist, A. Hjortsberg, Radiative cooling to low temperatures: General considerations and application to selectively emitting SiO films. *Journal of Applied Physics*. **52**, 4205–4220 (1981).

2. S. D. Lord, "A new software tool for computing Earth's atmospheric transmission of near- and far-infrared radiation" (1992), (available at https://ntrs.nasa.gov/search.jsp?R=19930010877).

3. A. L. Buck, New Equations for Computing Vapor Pressure and Enhancement Factor. *J. Appl. Meteor*. **20**, 1527–1532 (1981).